



Royal Netherlands Institute for Sea Research

This is a postprint of:

Weijers, J.W.H., Schefuß, E., Kim, J.-H., Sinninghe Damsté, J.S., & Schouten, S. (2014). Constraints on the sources of branched tetraether membrane lipids in distal marine sediments. *Organic Geochemistry*, 72, 14-22

Published version: dx.doi.org/10.1016/j.orggeochem.2014.04.011

Link NIOZ Repository: www.vliz.be/nl/imis?module=ref&refid=240760

[Article begins on next page]

The NIOZ Repository gives free access to the digital collection of the work of the Royal Netherlands Institute for Sea Research. This archive is managed according to the principles of the [Open Access Movement](#), and the [Open Archive Initiative](#). Each publication should be cited to its original source - please use the reference as presented.

When using parts of, or whole publications in your own work, permission from the author(s) or copyright holder(s) is always needed.

Constraints on the sources of branched tetraether membrane lipids in distal marine sediments

Johan W.H. Weijers^{a,1,2}, Enno Schefuß^b, Jung-Hyun Kim^c, Jaap S. Sinninghe Damsté^{a,c} and Stefan Schouten^{a,c}

^a*Utrecht University, Department of Earth Sciences – Geochemistry, Budapestlaan 4, 3584 CD Utrecht, The Netherlands*

^b*MARUM – Center for Marine Environmental Sciences, University of Bremen, Leobener Strasse, D-28359 Bremen, Germany (schefuss@uni-bremen.de)*

^c*NIOZ Royal Netherlands Institute for Sea Research, Department of Marine Organic Biogeochemistry, PO Box 59, 1790 AB Den Burg, The Netherlands (Jung-Hyun.Kim@nioz.nl; Jaap.Damste@nioz.nl; Stefan.Schouten@nioz.nl)*

¹Present address: Shell Global Solutions International B.V., Kessler Park 1, 2288 GS Rijswijk, The Netherlands (johan.weijers@shell.com)

²Corresponding author (johan.weijers@shell.com; phone: +31-70-4476229)

1 **Abstract**

2

3 Branched glycerol dialkyl glycerol tetraethers (brGDGTs) are membrane lipids produced by soil
4 bacteria and occur in near coastal marine sediments as a result of soil organic matter input. Their
5 abundance relative to marine-derived crenarchaeol, quantified in the BIT index, generally
6 decreases off-shore. However, in distal marine sediments, low relative amounts of brGDGTs can
7 often still be observed. Sedimentary in-situ production as well as dust input has been suggested
8 as potential, though as yet not well constrained, sources. In this study brGDGT distributions in
9 dust are examined and compared with those in distal marine sediments. Dust was sampled along
10 the equatorial West African coast and brGDGTs were detected in most of the samples, albeit in
11 low abundance. Their degree of methylation and cyclisation, expressed in the MBT'
12 (methylation index of branched tetraethers) and DC (degree of cyclisation) indices, respectively,
13 were comparable to those found for African soils, their presumed source. Comparison of DC
14 indices of brGDGTs in global soils, Congo deep-sea river fan sediments and dust with those of
15 distal marine sediments, however, clearly shows that distal marine sediments yield significantly
16 higher DC indices. This distinctive distribution is suggestive of sedimentary in-situ production as
17 source of brGDGTs in marine sediments, rather than dust input. The presence of in-situ produced
18 brGDGTs in marine sediments means that caution should be exercised when applying the MBT'-
19 CBT palaeothermometer in sediments with low BIT indices, i.e. <0.1 based on our dataset.

20

21

22 **Keywords:** Branched Tetraether; Dust; Marine Surface Sediment

23 1. Introduction

24

25 Marine sediments provide a unique archive to study Earth's past environment and climate.
26 Depending on the proximity of the study location to land, a varying proportion of the organic
27 matter (OM) input in marine sediments may be land derived. This terrigenous OM can be
28 delivered to marine sediments by several modes of transport, i.e. eolian dust input, suspended in
29 river water, or by means of gravity transport over the sea bed like through deep sea canyons or in
30 turbidites. Several proxies have been developed that try to distinguish between marine and
31 terrigenous derived OM. These can be either based on bulk properties like the C:N ratio and the
32 stable carbon isotopic ($\delta^{13}\text{C}$) composition of OM (Hedges et al., 1997 and references therein), or
33 based on the molecular composition, e.g. the (relative) abundance of lignin phenols (e.g. Goñi et
34 al., 1997) or other land specific biomarkers like long chain plant-wax derived *n*-alkanes
35 (Eglinton et al., 1962) or taraxerol (Killops and Frewin, 1994; Versteegh et al., 2004).

36

37 More recently, branched Glycerol Dialkyl Glycerol Tetraether (brGDGT) membrane lipids (Fig.
38 1) have been used as terrigenous biomarkers in marine sediments as they derive from soil
39 bacteria, likely belonging to the phylum of Acidobacteria (Sinninghe Damsté et al., 2000, 2011;
40 Weijers et al., 2006b, 2009a), and since their abundance in marine sediments quickly decreases
41 with increasing distance from the coast (Hopmans et al., 2004; Kim et al., 2006; Herfort et al.,
42 2006). Hopmans et al. (2004) proposed the Branched vs. Isoprenoid Tetraether (BIT) index to
43 quantify the relative abundance of these brGDGTs in marine sediments by normalising them to
44 crenarchaeol, an isoprenoid GDGT membrane lipid derived from ubiquitous pelagic
45 Thaumarchaeota (Sinninghe Damsté et al., 2002). It was suggested that this BIT index can be

46 used as proxy to trace terrigenous OM input into marine sediments (Hopmans et al., 2004).
47 However, subsequent studies demonstrated that the BIT index actually traces soil rather than
48 terrigenous OM input relative to marine OM input in near coastal marine sediments as brGDGTs
49 are present in soils and not in vegetation (Huguet et al., 2007; Walsh et al., 2008; Kim et al.,
50 2009; Weijers et al., 2009b; Smith et al., 2012).

51
52 Besides information on soil OM input, brGDGT distributions also provide information on
53 climate conditions on land. BrGDGTs vary in the number of methyl groups at the C5 and C5'
54 position (and recently it has been shown that methylation at the C6 and C6' position also occurs;
55 De Jonge et al., 2013), and contain one or two cyclopentane moieties (Weijers et al., 2006a). In a
56 set of soils obtained from across the globe, it was found that the degree of cyclisation, expressed
57 in the Cyclisation ratio of Branched Tetraethers (CBT), shows a strong relation with soil pH, and
58 the degree of branching, expressed in the Methylation index of Branched Tetraethers (MBT),
59 shows a strong relation with both soil pH and annual Mean Air Temperature (MAT, Weijers et
60 al., 2007b). Upon transport of brGDGTs to the marine environment and deposition in the marine
61 sedimentary archive, their distribution could hence be used to reconstruct past soil pH and past
62 annual MAT using these parameters in the so-called MBT-CBT proxy (e.g. Weijers et al.,
63 2007a). Recently the MBT index has been slightly modified (referred to as MBT') by excluding
64 two brGDGTs from analysis that usually occur in low abundance (i.e. <1 % of total brGDGTs) in
65 soils (Peterse et al., 2012). That same study also provided a new calibration for the MBT'-CBT
66 annual MAT proxy using this MBT' and based on a larger number of soils. In addition to the
67 CBT ratio, Sinninghe Damsté et al. (2009) introduced the degree of cyclisation (DC) index in

68 order to define the degree of cyclisation of brGDGTs in a similar way as the degree of
69 methylation in the MBT index, enabling a more direct comparison between the two.
70

71 Application of the BIT index and the MBT'-CBT proxy in marine sediments works under the
72 assumption that crenarchaeol is produced in the marine realm and brGDGTs are derived from
73 land. It has, however, been shown that Thaumarchaeota also thrive in soils, peat, lakes and river
74 water and hence that crenarchaeol is produced in these environments as well (e.g. Weijers et al.,
75 2004, 2006b; Powers et al., 2004; Leininger et al., 2006; Bannert et al., 2011; Zell et al., 2013).
76 The amount of crenarchaeol in soil and peat is, however, generally low relative to brGDGTs
77 causing soils and peat to be, on average, still characterised by a high BIT index value though
78 rarely reaching a value of 1 (0.90 on average; Schouten et al., 2013a and references cited
79 therein). A similar situation is observed in marine settings: although the BIT index in distal
80 marine settings is often low, it seldom reaches a value of 0 (average 0.04; Schouten et al., 2013a)
81 as in most distal marine sediments small amounts of brGDGTs remain detectable. The sources of
82 these brGDGTs are uncertain. Long distance dust transport over the oceans might be a plausible
83 mechanism for delivery of brGDGTs to remote ocean settings and brGDGTs have indeed been
84 reported in atmospheric dust sampled off northwest Africa (Fietz et al., 2013). Alternatively,
85 brGDGTs could be produced in-situ in marine sediments as suggested for near shore marine
86 sediments in a Svalbard fjord (Peterse et al., 2009) and in East China Sea sediments (Zhu et al.,
87 2011) based on differences in brGDGT distributions in marine sediments vs. soils on adjacent
88 land. However, it remains unclear to what extent these findings represent local, near coastal in-
89 situ production, or that marine in-situ production of brGDGTs is a more general phenomenon.
90

91 To investigate whether dust or in-situ production is responsible for the presence of brGDGTs in
92 distal marine sediments, we analysed the distribution of brGDGTs in atmospheric dust and
93 marine surface waters from the coast of western Africa and in globally distributed open ocean
94 sediments. These data are compared with previously published brGDGT distributions from the
95 western African Congo deep sea river fan sediments and with global soils in order to constrain
96 the potential source of brGDGTs in distal marine sediments and to identify potential implications
97 for the use of GDGT-based proxies.

98

99 **2. Material and methods**

100 *2.1. Samples*

101 Atmospheric dust was sampled along the west coast of equatorial Africa onboard the R/V Meteor
102 cruise M41/1 in 1998. Details on sampling and extraction procedures are provided by Schefuß et
103 al. (2003). For the present study, polar fractions of lipid extracts from 13 dust filters (Table 1;
104 Fig. 2) were dried, redissolved in *n*-hexane:*iso*-propanol 99:1 (v/v), and filtered through a 0.45
105 µm mesh PTFE filter prior to analysis of their GDGT content.

106 Suspended particulate matter (SPM) in marine surface waters was sampled by filtration of ca.
107 100 to 400 L water, provided by the ship's seawater inlet (ca. 5 m water depth), through a 0.7 µm
108 GFF filter onboard R/V Meteor during cruise M56 in December 2002 along the west coast of
109 equatorial Africa (Spiess and Cruise Participants, 2008). The eight sampling locations comprise a
110 transect along the equatorial African coast and include the lower salinity (down to 28.0 ‰)
111 Congo River outflow plume (Table 2; Fig. 2). Filters were freeze dried, cut into small pieces and
112 extracted using a dichloromethane (DCM):methanol (MeOH) 9:1 (v/v) mixture using accelerated
113 solvent extraction (Dionex ASE 200, 100°C, 1000 psi, 3 cycles of 5 min). The obtained total

114 lipid extract was saponified with 6% KOH (2 h at 85°C) and the extracted neutral fraction was
115 dried and separated over pre-combusted silica gel columns into an apolar, a ketone, and a polar
116 fraction using *n*-hexane, DCM, and DCM:MeOH 1:1 (v/v) solvent mixtures, respectively.
117 Further preparation of the polar fractions was similar to that of the dust samples.
118 A total of 34 distal marine surface sediments (Table 3) were analysed for their brGDGT content.
119 These sediments were selected from the core-top calibration data set used for the TEX₈₆ sea
120 surface temperature proxy, based on their low BIT index, i.e. <0.03 (Schouten et al., 2002; Kim
121 et al., 2008, 2010). The polar fractions of the selected samples were obtained as described
122 previously (Schouten et al., 2002; Kim et al., 2008, 2010) and analysed for their brGDGT
123 content. The small differences in extraction techniques and clean up procedures between the
124 sample sets are not expected to influence the GDGT distributions. Previous studies have shown
125 that the type of extraction method and extract processing have not a large effect on the GDGT
126 distributions (Schouten et al., 2007; Escala et al., 2009; Lengger et al., 2012) and that differences
127 remain within repeatability limits (Schouten et al., 2013b).

128

129 2.2. GDGT analysis

130 Samples were analysed for their GDGT content using High Performance Liquid
131 Chromatography / Atmospheric Pressure Chemical Ionization – Mass Spectrometry
132 (HPLC/APCI-MS) on an Agilent 1100 series instrument equipped with Chemstation software
133 according to Schouten et al. (2007). Separation of compounds was achieved on an analytical
134 Alltech Prevail Cyano column (150 mm x 2.1 mm; 3µm) held at a constant 30°C and using *n*-
135 hexane:*iso*-propanol 99:1 (v/v) as eluent, isocratically for the first 5 min, then increasing to 1.8%
136 *iso*-propanol in 45 min. The column was rinsed in back flush mode with 10% *iso*-propanol in *n*-

137 hexane and re-equilibrated to starting conditions after each run. GDGTs were analysed in
138 Selective Ion Monitoring (SIM) mode as their $[M+H]^+$ (protonated) derivatives. Relative
139 quantification of the GDGTs was based on peak areas in the $[M+H]^+$ mass chromatograms. The
140 BIT index was used as defined by Hopmans et al. (2004):

141

$$142 \quad BIT = \frac{[Ia + IIa + IIIa]}{[Ia + IIa + IIIa + IV]} \quad (1)$$

143

144 The MBT' index was used as defined by Peterse et al. (2012) and differs from the original
145 definition (Weijers et al., 2007b) in the omission of GDGTs IIIb and IIIc:

146

$$147 \quad MBT' = \frac{[Ia + Ib + Ic]}{[Ia + Ib + Ic + IIa + IIb + IIc + IIIa]} \quad (2)$$

148

149 The degree of cyclisation (DC) of brGDGTs was used as defined by Sinninghe Damsté et al.
150 (2009):

151

$$152 \quad DC = \frac{[Ib + IIb]}{[Ia + Ib + IIa + IIb]} \quad (3)$$

153

154 The CBT ratio was used as defined by Weijers et al. (2007b):

155

$$156 \quad CBT = -\log \left(\frac{[Ib + IIb]}{[Ia + IIa]} \right) \quad (4)$$

157

158 Roman numerals refer to the structures given in Fig. 1.

159

160 *2.3. Statistical analysis*

161 An analysis of variance (ANOVA) was conducted on the DC and MBT' indices of different
162 sample groups to determine whether or not these differ significantly from each other. The
163 analysis was carried out by means of a pairwise multiple comparison test using Tamhane's T2
164 procedure, which assumes no equal variance between sample groups. Statistical analyses were
165 conducted using the SPSS 21.0 software package (IBM corp.).

166

167 **3. Results and discussion**

168 *3.1. Atmospheric dust as a potential source for brGDGTs in the marine environment*

169 HPLC-MS analysis of the dust sampled along the African coast (Fig. 2) showed the presence of
170 brGDGTs in all but one sample. However, none of the dust samples contained the full suite of
171 brGDGTs, i.e. GDGTs IIIb and IIIc were not detected in any of the dust samples. Only in 5 out
172 of the 13 dust samples all brGDGTs necessary for calculating a DC index and CBT ratio were
173 present above detection level (Table 1). In a previous study, the analysis of two dust samples
174 obtained from the same area as the dust filters analysed here did not yield any brGDGT signal
175 (Hopmans et al., 2004), making the authors to suggest that brGDGTs are barely, if at all,
176 transported by dust. The mass spectrometer in that analysis, however, was set to scan ions over
177 the range m/z 950 to 1450, i.e. in 'full scan' mode. The extracts of dust samples in the present
178 study were run in the more sensitive Selective Ion Monitoring (SIM) mode, scanning only for the
179 masses of interest, thereby increasing the sensitivity for GDGT detection by one to two orders of
180 magnitude (cf. Schouten et al., 2007). This likely explains why at least some brGDGTs are now

181 detected in dust and this implies that dust could be a potential source of brGDGTs in distal
182 marine sediments. This corroborates a recent publication by Fietz et al. (2013) that reports
183 brGDGTs in dust sampled off northwest Africa.

184 Backward trajectories for the dust samples used in our study have been computed previously
185 (Schefuß et al., 2003) and indicate that air masses sampled on the filters mostly originate from
186 the nearby African continent, especially from the Faya Largeau region in Chad. Therefore, it
187 could be assumed that the brGDGTs in the dust are derived from nearby African soils and thus
188 that their distributions, as expressed in the degrees of methylation and cyclisation (MBT' and
189 DC), should be similar to those of African soils. The average MBT' and DC indices for
190 brGDGTs in the dust samples are $0.80 (\pm 0.06; n=8)$ and $0.11 (\pm 0.04; n=5)$, respectively (Table
191 1). This falls within the range of African soils (from the soil database in Peterse et al., 2012), i.e.
192 $0.76 (\pm 0.22; n=12)$ and $0.13 (\pm 0.18; n=16)$ for MBT' and DC, respectively, although the
193 variation in soils is larger (Fig. 3). Furthermore, the MBT' and DC indices of the dust are similar
194 to previously reported MBT' and DC indices of brGDGTs present in the surface sediments from
195 the Congo deep sea river fan (Weijers et al., 2007a), i.e. $0.72 (\pm 0.10; n=7)$ and $0.15 (\pm 0.08; n=7)$,
196 Table 4, Fig. 3). This indeed suggests that brGDGTs found in the dust are ultimately derived
197 from soils on the adjacent African continent.

198 Notably, however, crenarchaeol was detected in all of the 13 dust samples and BIT indices
199 determined for the dust are substantially lower (average 0.25 ± 0.08 , $n=12$; Table 1) compared to
200 values generally found in soils, e.g. the average BIT index value in a compilation of global soil
201 data by Schouten et al. (2013a) is $0.90 (\pm 0.14; n=224)$ with only a minority of soils having BIT
202 index values < 0.5 . Indeed, BIT indices for dust are also clearly lower than BIT indices for
203 African soils reported in Peterse et al. (2012), which are on average $0.81 (\pm 0.21; n=16)$. The

204 latter dataset only contains two soils with BIT <0.50 and none reaching as low as 0.25. These
205 differences could be caused by two processes, i.e. selective degradation of GDGTs during
206 atmospheric transport or addition of crenarchaeol to dust. Selective degradation of brGDGTs
207 relative to crenarchaeol during atmospheric dust transport seems unlikely. Huguet et al. (2008)
208 have shown that in a turbidite deposit subject to prolonged oxygen exposure, crenarchaeol is
209 preferentially oxidized compared to brGDGTs. This was attributed, however, to the fact that the
210 terrigenous derived brGDGTs were likely protected via close association with clay minerals in
211 contrast to the marine-derived crenarchaeol. If derived from soils, crenarchaeol will be similarly
212 associated with dust particles as brGDGTs and therefore no selective degradation is expected.
213 Hence, there may be an additional source for crenarchaeol to explain the low BIT indices for
214 dust. One likely source for additional crenarchaeol on the dust filters is sea spray. Indeed,
215 analysis of the surface waters collected along the western African coast showed the clear
216 presence of crenarchaeol (Table 2) pointing to sea spray as a potential source of crenarchaeol. In
217 some of the surface waters brGDGTs were also detected, suggesting that sea spray may also be a
218 source for the brGDGTs on the dust filters. However, only the surface waters from the lower
219 salinity waters of the Congo River plume contain brGDGTs, likely delivered by the Congo River
220 (cf. Hopmans et al., 2004; Weijers et al., 2007a). In contrast, surface waters taken outside the
221 Congo River plume area barely contain brGDGTs, if at all (Table 2). Hence, the brGDGTs
222 detected in the dust, sampled outside areas of major river influence, are suggested to be
223 predominantly sourced by particles derived from the African continent. Notably, the dust
224 sampled off northwest Africa by Fietz et al. (2013) reflected BIT index values of 0.84 on
225 average. Although BIT index analyses between laboratories could differ substantially (Schouten
226 et al., 2013b), this still is a large difference. As yet it is difficult to explain this difference, but

227 maybe the location of the dust samplers on the research vessel, i.e. their proximity to the sea
228 surface, and weather conditions, might play a role here.

229

230 *3.2. Sources of brGDGTs in distal marine sediments*

231 Transport of dust from the African continent to the equatorial Atlantic oceans is a well-known
232 phenomenon (e.g. Darwin, 1846; Chester et al., 1972; Prospero and Carlson, 1972) and for plant
233 wax derived long chain *n*-alkanes it has been shown that they can be delivered to the marine
234 realm via dust transport over distances of several thousand kilometres (e.g. Simoneit, 1977;
235 Gagosian et al., 1981; Schefuß et al., 2003; Bendle et al. 2007) and recently Fietz et al. (2013)
236 showed the presence of brGDGTs in dust far off northwest Africa. In order to see if also an
237 important contributor to the pool of brGDGTs in distal marine sediments, we compare
238 distributions of brGDGTs in both African soils and near shore dust with those in low latitude
239 Atlantic Ocean surface sediments (Table 3 and Fig. 2). Analysis shows that all Atlantic Ocean
240 surface sediments contained brGDGTs, though one sediment did not contain all brGDGTs in
241 sufficient amounts for calculating a DC index (Table 3). The MBT' index of these Atlantic
242 Ocean sediments is on average 0.28 (± 0.10 ; $n=9$, Table 5). This is significantly different
243 ($p<0.001$) from MBT' indices of African soils and dust, i.e. 0.76 (± 0.22 , $n=16$) and 0.80 (± 0.06 ,
244 $n=8$) on average, respectively (Tables 5 and 6). Although this could potentially indicate that
245 brGDGTs in these sediments are not derived from the warm African continent but derived from
246 higher and thus colder latitudes with lower MBT' values, this seems unlikely as Africa is the
247 major source of dust in the Atlantic Ocean (e.g. Schefuß et al., 2003 and references cited therein;
248 Fietz et al., 2013). When DC indices of African soils and dust are compared with those of low
249 latitude Atlantic surface sediments, a similar pattern emerges as for the MBT': DC indices of

250 equatorial Atlantic sediments are on average $0.39 (\pm 0.16, n=8)$, which is significantly different
251 ($p < 0.10$) from that of African soils and dust, i.e. $0.13 (\pm 0.18, n=16)$ and $0.11 (\pm 0.04, n=5)$,
252 respectively (Tables 5 and 6, Fig. 4). Collectively, these differences in distribution strongly
253 suggest that brGDGTs in the low latitude Atlantic sediments are not primarily sourced by
254 African dust.

255 In addition to the low-latitude Atlantic Ocean sediments, a set of 25 distal marine sediments from
256 other locations were analysed for their brGDGT distribution (Table 3). Four additional open
257 marine sediments characterised by a low BIT index (i.e. < 0.08), and for which brGDGT
258 composition was previously reported by Peterse et al. (2009) and Zhu et al. (2011), were added
259 to the dataset as well to make a total of 38 marine sediments, including the low latitude Atlantic
260 Ocean sediments. Out of these 38 sediments, 35 contained sufficient amounts of brGDGTs
261 required for calculating a DC index (Table 3). The average value of the DC indices for these
262 distal marine sediments is $0.40 (\pm 0.16, n=35)$. This is similar to the average value as found for
263 the low-latitude Atlantic sediments, but significantly different ($p < 0.10$) from DC indices of
264 global soils (Tables 5 and 6, Fig. 4). Thus, it can be concluded that also on a more global scale
265 the distribution of brGDGTs in distal marine sediments is significantly different from the
266 distribution of brGDGTs in terrigenous sources and, hence, that dust input is likely not a major
267 source for them. The alternative explanation is that brGDGTs in open marine sediments are
268 produced in-situ. For near coastal locations, in-situ production has been suggested previously by
269 Peterse et al. (2009) and Zhu et al. (2011) and, interestingly, these studies reported distinctively
270 high degrees of cyclisation (i.e. low CBT ratios) for marine sediments as well. Peterse et al.
271 (2009) found that marine and fjord sediments around Svalbard were characterised by an average
272 CBT ratio of $-0.27 (\pm 0.09)$, which equals an average DC index of $0.65 (\pm 0.03)$, much higher than

273 the average DC index of Svalbard soils of 0.17 (± 0.11). Zhu et al. (2011) found increased
274 brGDGT abundances normalised on TOC further away from the river mouth onto the shelf,
275 which is accompanied by a trend to higher DC indices (Fig. 5, based on data reported in Zhu et
276 al., 2011). In addition, brGDGTs have been reported in sediments at and near hydrothermal vents
277 along the Eastern Lau Spreading Center in the South Pacific Ocean (Hu et al., 2012) and two
278 types of brGDGTs have been reported in a carbonate chimney of Lost City Hydrothermal Field
279 near the mid-Atlantic Ridge (Lincoln et al., 2013). Notably, based on the data provided in Hu et
280 al. (2012), the brGDGTs in their sediment TVG8 are also characterised by a high degree of
281 cyclisation. Our results, together with those of Peterse et al. (2009) and Zhu et al. (2011), as well
282 as Hu et al. (2012) and Lincoln et al. (2013), form strong circumstantial evidence for the global
283 occurrence of in-situ production of brGDGTs in marine sediments. For soils and peat it has been
284 suggested that Acidobacteria might be the dominant producers of brGDGTs (Weijers et al.,
285 2009a; Sinninghe Damsté et al., 2011). Although a microbial community producing brGDGTs in
286 the marine environment might be totally different from that in soils, Acidobacteria have indeed
287 been reported to be present in marine surface sediments as well as in hydrothermal chimneys
288 (Barns et al., 1999; Lopez-Garcia et al., 2003, Polymenakou et al., 2005; Li et al., 2009;
289 Brazelton et al., 2010).

290

291 *3.3. Exploring factors controlling the distribution of marine brGDGTs*

292 As discussed in section 3.2, brGDGTs present in open marine sediments are characterised by
293 relatively high DC and low CBT values. In soils the CBT ratio of brGDGTs is related to soil pH
294 (Weijers et al., 2007b; Peterse et al., 2010) with a higher degree of cyclisation (equals low CBT
295 ratios) corresponding to higher pH values. When the marine CBT values are translated to pH

296 using the global soil calibration (Weijers et al., 2007b), reconstructed pH varies between 6.1 and
297 9.9. Although this includes the average ocean water pH of ca. 8, the variability is large in
298 comparison with the relatively small variation in sea water pH. This large variation in DC indices
299 may indicate that the brGDGTs found in marine sediments are mainly produced within these
300 sediments, where pH values can rapidly change depending on redox conditions, rather than in the
301 marine water column. Unfortunately, no long term pH data are available for the core top
302 sediments used in this study to investigate the relation between the degree of cyclisation and
303 sediment pH in more detail.

304

305 *3.4. Implications for GDGT based proxies*

306 The production of brGDGTs in marine sediments may have consequences for some of the
307 GDGT-based proxies currently used. For example, the BIT index is used as indicator for the
308 relative amount of soil OM in marine sediments (Hopmans et al., 2004). Due to the relatively
309 small amounts of brGDGTs found in distal marine sediments the marine end-member of the BIT
310 index will be slightly higher than 0. Indeed, based on a data compilation, Schouten et al. (2013a)
311 found an average BIT index for open marine sediments of 0.04 (± 0.03 , $n=278$). However, as the
312 end-member distributions for soils (0.90 ± 0.14 , $n=224$; Schouten et al. 2013a) and marine
313 sediments are still substantially different, marine in-situ produced brGDGTs will not
314 substantially influence the use of the BIT index in marine sediments as indicator of soil derived
315 OM.

316 The MBT'-CBT proxy is used to estimate past continental air temperatures based on the
317 distribution of soil-derived brGDGTs (Weijers et al., 2007b; Peterse et al., 2012). It is applied in
318 marine sediments that receive substantial soil OM input, and thus characterised by a high BIT

319 index, preferably near river outflows in order to obtain river-basin integrated signals (Weijers et
320 al., 2007a). This study shows that at low BIT indices, the MBT' index and CBT ratio become
321 skewed by the ostensibly marine in-situ produced brGDGTs and, therefore, render the MBT'-
322 CBT proxy unsuitable. Sites characterised by low BIT indices not only include distal marine
323 settings but also coastal settings removed from any fluvial OM input. In our dataset of Congo
324 deep sea river fan sediments, one location with a low BIT index of 0.05 (T89-14) yields a DC
325 index clearly higher (and consequently a CBT ratio clearly lower) than the other Congo deep sea
326 fan sediments that are characterised by a higher BIT index (Table 4). In the East China Sea
327 dataset of Zhu et al. (2011) the sediments with elevated DC indices, i.e. >0.35 (Fig. 5) have an
328 average BIT index of 0.09 (± 0.02 , n=12). Based on these data, therefore, a BIT index threshold
329 of >0.1 seems appropriate for MBT'-CBT applications. It needs to be emphasized, however, that
330 at other locations this threshold might be somewhat higher, for example due to lower
331 crenarchaeol production. Although a previous interlaboratory study highlighted concerns
332 regarding the reproducibility of the BIT index between laboratories and instruments (Schouten et
333 al., 2009), a recent and more extensive interlaboratory comparison showed that low BIT indices
334 (i.e. <0.1) can be reproduced relatively precisely between laboratories (Schouten et al., 2013b).
335 Since variations in terrigenous soil OM input also occur over time, down core MBT'-CBT
336 applications should always be accompanied with a BIT index record.

337

338 **4. Conclusions**

339 Our study shows that brGDGTs are present in dust, albeit in low abundance. Distributions of
340 dust-derived brGDGTs are similar to those of soils but clearly different from those of distal
341 marine sediments. Thus, although dust input to open ocean settings might occur, it does not seem

342 to be an important source of brGDGTs in distal marine settings. Branched GDGT distributions in
343 distal marine sediments are characterised by a distinctive high DC index. This strongly suggests
344 in-situ production of brGDGTs in distal marine sediments on a global scale, and supports earlier
345 reports of potential in-situ production in near coastal marine sediments (Peterse et al., 2009; Zhu
346 et al., 2011). Based on the large variability of DC indices in marine sediments, it is suggested
347 that marine derived brGDGTs are mainly produced in-situ in the sediments rather than the
348 overlying water column. The magnitude of in-situ production of brGDGTs is low compared to
349 pelagic marine crenarchaeol production and, therefore, not notably influencing the use of the BIT
350 index as proxy for relative soil OM input in marine sediments. However, the MBT'-CBT proxy
351 for continental temperatures will be biased by in-situ produced brGDGTs when the overall
352 abundance of brGDGTs is low, i.e. at low BIT indices (based on data in this study <0.1). It
353 should therefore only be applied to settings known to receive substantial soil OM input.

354

355 **Acknowledgements**

356 The authors wish to thank Chun Zhu and Francien Peterse for sharing GDGT data from the East
357 China Sea and the global soil dataset. Gert-Jan Reichart is thanked for helpful discussion. We
358 thank the Captain and crew of R/V Meteor for enabling the seawater sampling during M56. Two
359 anonymous reviewers and the editor are thanked for their comments which helped to improve
360 this manuscript. The work leading to these results has received partial funding from the
361 European Research Council under the European Union's Seventh Framework Programme
362 (FP/2007-2013) / ERC Grant Agreement nr. 226600 to J.S.S.D. and nr. 306390 to J.W.H.W..
363 Both J.W.H.W. and S.S. thank the Netherlands Organisation for Scientific Research (NWO) for
364 funding through a Veni and Vici grant, respectively.

References

- Bannert, A., Mueller-Niggemann, C., Kleineidam, K., Wissing, L., Cao, Z.H., Schwark, L., Schloter, M., 2011. Comparison of lipid biomarker and gene abundance characterizing the archaeal ammonia-oxidizing community in flooded soils. *Biology and Fertility of Soils* 47, 839-843.
- Barns, S.M., Takala, S.L., Kuske, C.R., 1999. Wide distribution and diversity of members of the bacterial Kingdom Acidobacterium in the environment. *Applied and Environmental Microbiology* 65, 1731-1737.
- Bendle, J., Kawamura, K., Yamazaki, K., Niwai, T., 2007. Latitudinal distribution of terrestrial lipid biomarkers and *n*-alkane compound-specific stable carbon isotope ratios in the atmosphere over the western Pacific and Southern Ocean. *Geochimica et Cosmochimica Acta* 71, 5934-5955.
- Brazelton, W.J., Ludwig, K.A., Sogin, M.L., Andreishcheva, E.N., Kelley, D.S., Shen, C.-C., Edwards, R.L., Baross, J.A., 2010. Archaea and bacteria with surprising microdiversity show shifts in dominance over 1,000-year time scales in hydrothermal chimneys. *Proceedings of the National Academy of Sciences of the USA* 107, 1612-1617.
- Chester, R., Elderfield, H., Griffin, J.J., Johnson, L.R., Padgham, R.C., 1972. Eolian dust along the eastern margins of the Atlantic Ocean. *Marine Geology* 13, 91-105.
- Darwin, C., 1846. An account of the fine dust which often falls on vessels in the Atlantic Ocean. *Quarterly Journal of the Geological Society* 2, 26-30.
- De Jonge, C., Hopmans, E.C., Stadnitskaia, A., Rijpstra, W.I.C., Hofland, R., Tegelaar, E., Sinninghe Damsté, J.S., 2013. Identification of novel penta- and hexamethylated branched glycerol dialkyl glycerol tetraethers in peat using HPLC-MS², GC-MS and GC-SMB-MS. *Organic Geochemistry* 54, 78-82.
- Eglinton, G., Gonzalez, A.G., Hamilton, R.J., Raphael, R.A., 1962. Hydrocarbon constituents of the wax coatings of plant leaves - a taxonomic survey. *Phytochemistry* 1, 89-102.
- Escala, M., Fietz, S., Rueda, G., Rosell-Melé, A., 2009. Analytical considerations for the use of the paleothermometer Tetraether Index 86 and the branched vs isoprenoid tetraether index regarding the choice of cleanup and instrumental conditions. *Analytical Chemistry* 81, 2701-2707.
- Fietz, S., Prahl, F.G., Moraleda, N., Rosell-Melé, A., 2013. Eolian transport of glycerol dialkyl glycerol tetraethers (GDGTs) off northwest Africa. *Organic Geochemistry* 64, 112-118.
- Gagosian, R.B., Peltzer, E.T., Zafiriou, O.C., 1981. Atmospheric transport of continentally derived lipids to the tropical north Pacific. *Nature* 291, 312-315.
- Goñi, M.A., Ruttenger, K.C., Eglinton, T.I., 1997. Source and contribution of terrigenous organic carbon to surface sediments in the Gulf of Mexico. *Nature* 389, 275-278.

- Hedges, J.I., Keil, R.G., Benner, R., 1997. What happens to terrestrial organic matter in the ocean? *Organic Geochemistry* 27, 195-212.
- Herfort, L., Schouten, S., Boon, J.P., Woltering, M., Baas, M., Weijers, J.W.H., Sinninghe Damsté, J.S., 2006. Characterization of transport and deposition of terrestrial organic matter in the southern North Sea using the BIT index. *Limnology and Oceanography* 51, 2196-2205.
- Hopmans, E.C., Weijers, J.W.H., Schefuß, E., Herfort, L., Sinninghe Damsté, J.S., Schouten, S., 2004. A novel proxy for terrestrial organic matter in sediments based on branched and isoprenoid tetraether lipids. *Earth and Planetary Science Letters* 224, 107-116.
- Hu, J., Meyers, P.A., Chen, G., Peng, P., Yang, Q., 2012. Archaeal and bacterial glycerol dialkyl glycerol tetraethers in sediments from the Eastern Lau Spreading Center, South Pacific Ocean. *Organic Geochemistry* 43, 162-167.
- Huguet, C., de Lange, G.J., Gustafsson, Ö., Middelburg, J.J., Sinninghe Damsté, J.S., Schouten, S., 2008. Selective preservation of soil organic matter in oxidized marine sediments (Madeira Abyssal Plain). *Geochimica et Cosmochimica Acta* 72, 6061-6068.
- Huguet, C., Smittenberg, R.H., Boer, W., Sinninghe Damsté, J.S., Schouten, S., 2007. Twentieth century proxy records of temperature and soil organic matter input in the Drammensfjord, southern Norway. *Organic Geochemistry* 38, 1838-1849.
- Killops, S.D., Frewin, N.L., 1994. Triterpenoid diagenesis and cuticular preservation. *Organic Geochemistry* 21, 1193-1209.
- Kim, J.-H., Schouten, S., Hopmans, E.C., Donner, B., Sinninghe Damsté, J.S., 2008. Global sediment core-top calibration of the TEX86 paleothermometer in the ocean. *Geochimica et Cosmochimica Acta* 72, 1154-1173.
- Kim, J.-H., van der Meer, J., Schouten, S., Helmke, P., Willmott, V., Sangiorgi, F., Koc, N., Hopmans, E.C., Sinninghe Damsté, J.S., 2010. New indices and calibrations derived from the distribution of crenarchaeal isoprenoid tetraether lipids: Implications for past sea surface temperature reconstructions. *Geochimica et Cosmochimica Acta* 74, 4639-4654.
- Kim, J.-H., Buscail, R., Bourrin, F., Palanques, A., Sinninghe Damsté, J.S., Bonnin, J., Schouten, S., 2009. Transport and depositional process of soil organic matter during wet and dry storms on the Têt inner shelf (NW Mediterranean). *Palaeogeography, Palaeoclimatology, Palaeoecology* 273, 228-238.
- Kim, J.-H., Schouten, S., Buscail, R., Ludwig, W., Bonnin, J., Sinninghe Damsté, J.S., Bourrin, F., 2006. Origin and distribution of terrestrial organic matter in the NW Mediterranean (Gulf of Lion): application of the newly developed BIT index. *Geochemistry, Geophysics, Geosystems* 7, Q11017-[doi:10.1029/2006GC001306](https://doi.org/10.1029/2006GC001306).
- Leininger, S., Urich, T., Schloter, M., Schwark, L., Qi, J., Nicol, G.W., Prosser, J.I., Schuster, S. C., Schleper, C., 2006. Archaea predominate among ammonia-oxidizing prokaryotes in soils. *Nature* 442, 806-809.

- Lengger, S.K., Hopmans E.C., Sinninghe Damsté, J.S., Schouten, S., 2012. A comparison of extraction and work-up techniques for analysis of core- and intact polar tetraether lipids from sedimentary environments. *Organic Geochemistry* 47, 34-40.
- Li, H., Yu, Y., Luo, W., Zeng, Y., Chen, B., 2009. Bacterial diversity in surface sediments from the Pacific Arctic Ocean. *Extremophiles* 13, 233-246.
- Lincoln, S.A., Bradley, A.S., Newman, S.A., Summons, R.E., 2013. Archaeal and bacterial glycerol dialkyl glycerol tetraether lipids in chimneys of the Lost City Hydrothermal Field. *Organic Geochemistry* 60, 45-53.
- López-García, P., Duperron, S., Philippot, P., Foriel, J., Susini, J., Moreira, D., 2003. Bacterial diversity in hydrothermal sediment and epsilonproteobacterial dominance in experimental microcolonizers at the Mid-Atlantic Ridge. *Environmental Microbiology* 5, 961-976.
- Peterse, F., Kim, J.-H., Schouten, S., Klitgaard Kristensen, D., Koç, N., Sinninghe Damsté, J.S., 2009. Constraints on the application of the MBT/CBT palaeothermometer at high latitude environments (Svalbard, Norway). *Organic Geochemistry* 40, 692-699.
- Peterse, F., Nicol, G.W., Schouten, S., Sinninghe Damsté, J.S., 2010. Influence of soil pH on the abundance and distribution of core and intact polar lipid-derived branched GDGTs in soil. *Organic Geochemistry* 41, 1171-1175.
- Peterse, F., van der Meer, J., Schouten, S., Weijers, J.W.H., Fierer, N., Jackson, R.B., Kim, J.-H., Sinninghe Damsté, J.S., 2012. Revised calibration of the MBT-CBT paleotemperature proxy based on branched tetraether membrane lipids in surface soils. *Geochimica et Cosmochimica Acta* 96, 215-229.
- Polymenakou, P.N., Bertilsson, S., Tselepides, A., Stephanou, E.G., 2005. Bacterial community composition in different sediments from the Eastern Mediterranean Sea: a comparison of four 16S ribosomal DNA clone libraries. *Microbial Ecology* 50, 447-462.
- Powers, L.A., Werne, J.P., Johnson, T.C., Hopmans, E.C., Sinninghe Damsté, J.S., Schouten, S., 2004. Crenarchaeotal membrane lipids in lake sediments: A new paleotemperature proxy for continental paleoclimate reconstruction? *Geology* 32, 613-616.
- Prospero, J.M., Carlson, T.N., 1972. Vertical and areal distribution of Saharan dust over the western equatorial North Atlantic Ocean. *Journal of Geophysical Research* 77, 5255-5265.
- Schefuß, E., Ratmeyer, V., Stuut, J.-B.W., Jansen, J.H.F., and Sinninghe Damsté, J.S., 2003. Carbon isotope analyses of n-alkanes in dust from the lower atmosphere over the central eastern Atlantic. *Geochimica et Cosmochimica Acta* 67, 1757-1767.
- Schefuß, E., Versteegh, G.J.M., Jansen, J.H.F., Sinninghe Damsté, J.S., 2004. Lipid biomarkers as major source and preservation indicators in SE Atlantic surface sediments. *Deep-Sea Research I* 51, 1199-1228.

- Schouten, S., Hopmans, E.C., Sinninghe Damsté, J.S., 2013a. The organic geochemistry of glycerol dialkyl glycerol tetraether lipids: A review. *Organic Geochemistry* 54, 19-61.
- Schouten, S., Hopmans, E.C., Rosell-Melé, A., Pearson, A., Adam, P., Bauersachs, T., Bard, E., Bernasconi, S.M., Bianchi, T.S., Brocks, J.J., Carlson, L.T., Castañeda, I.S., Derenne, S., Dogrul Selver, A., Dutta, K., Eglinton, T., Fosse, C., Galy, V., Grice, K., Hinrichs, K.-U., Huang, Y., Huguet, A., Huguet, C., Hurley, S., Ingalls, A., Jia, G., Keely, B., Knappy, C., Kondo, M., Krishnan, S., Lincoln, S., Lipp, J., Mangelsdorf, K., Martínez-García, A., van der Meer, J., Ménot, G., Mets, A., Mollenhauer, G., Ohkouchi, N., Ossebaar, J., Pagani, M., Pancost, R.D., Pearson, E.J., Peterse, F., Reichart, G.-J., Schaeffer, P., Schmitt, G., Schwark, L., Shah, S.R., Smith, R.W., Smittenberg, R.H., Takano, Y., Talbot, H.M., Taylor, K.W.R., Tarazo, R., van Dongen, B.E., Van mooy, B.A.S., Wang, J., Warren, C., Weijers, J.W.H., Werne, J.P., Woltering, M., Xie, S., Yamamoto, M., Yang, H., Zhang, C.L., Zhang, Y., Zhao, M., Sinninghe Damsté, J.S., 2013b. An interlaboratory study of TEX₈₆ and BIT analysis of sediments, extracts and standard mixtures. *Geochemistry, Geophysics, Geosystems* 14, 5263-5285.
- Schouten, S., Hopmans, E.C., Schefuß, E., Sinninghe Damsté, J.S., 2002. Distributional variations in marine crenarchaeotal membrane lipids: a new tool for reconstructing ancient sea water temperatures? *Earth and Planetary Science Letters* 204, 265-274.
- Schouten, S., Hopmans, E.C., van der Meer, J., Mets, A., Bard, E., Bianchi, T.S., Diefendorf, A., Escala, M., Freeman, K.H., Furukawa, Y., Huguet, C., Ingalls, A., Ménot-Combes, G., Nederbragt, A.J., Oba, M., Pearson, A., Pearson, E.J., Rosell-Melé, A., Schaeffer, P., Shah, S.R., Shanahan, T.M., Smith, R.W., Smittenberg, R.H., Talbot, H.M., Uchida, M., Van mooy, B.A.S., Yamamoto, M., Zhang, Z., Sinninghe Damsté, J.S., 2009. An interlaboratory study of TEX₈₆ and BIT analysis using high-performance liquid chromatography-mass spectrometry. *Geochemistry, Geophysics, Geosystems* 10, Q03012, doi: 10.1029/2008GC002221.
- Schouten, S., Huguet, C., Hopmans, E.C., Kienhuis, M.V.M., Sinninghe Damsté, J.S., 2007. Analytical methodology for TEX₈₆ paleothermometry by high-performance liquid chromatography/atmospheric pressure chemical ionization-mass spectrometry. *Analytical Chemistry* 79, 2940-2944.
- Simoneit, B.R.T., 1977. Organic matter in eolian dusts over the Atlantic Ocean. *Marine Chemistry* 5, 443-464.
- Sinninghe Damsté, J.S., Hopmans, E.C., Pancost, R.D., Schouten, S., Geenevasen, J.A.J., 2000. Newly discovered non-isoprenoid glycerol dialkyl glycerol tetraether lipids in sediments. *Chemical Communications* 1683-1684.
- Sinninghe Damsté, J.S., Ossebaar, J., Abbas, B., Schouten, S., Verschuren, D., 2009. Fluxes and distribution of tetraether lipids in an equatorial African lake: Constraints on the application of the TEX₈₆ palaeothermometer and BIT index in lacustrine settings. *Geochimica et Cosmochimica Acta* 73, 4232-4249.
- Sinninghe Damsté, J.S., Rijpstra, W.I.C., Hopmans, E.C., Weijers, J.W.H., Foesel, B.U., Overmann, J., Dedysh, S.N., 2011. 13,16-Dimethyl octacosanedioic acid (iso-diabolic acid), a

- common membrane-spanning lipid of acidobacteria subdivisions 1 and 3. *Applied and Environmental Microbiology* 77, 4147-4154.
- Sinninghe Damsté, J.S., Schouten, S., Hopmans, E.C., van Duin, A.C.T., Geenevasen, J.A.J., 2002. Crenarchaeol: the characteristic core glycerol dibiphytanyl glycerol tetraether membrane lipid of cosmopolitan pelagic crenarchaeota. *Journal of Lipid Research* 43, 1641-1651.
- Smith, R.W., Bianchi, T.S., Li, X., 2012. A re-evaluation of the use of branched GDGTs as terrestrial biomarkers: Implications for the BIT Index. *Geochimica et Cosmochimica Acta* 80, 14-29.
- Spiess, V., Cruise Participants, 2008. Report and preliminary results of METEOR cruise M56, Douala - Cape Town, 20 November - 29 December 2002. METEOR - Berichte 08-1, Fachbereich Geowissenschaften, Universität Bremen, p.66.
- Versteegh, G.J.M., Schefuß, E., Dupont, L., Marret, F., Sinninghe Damsté, J.S., Jansen, J.H.F. 2004. Taraxerol and Rhizophora pollen as proxies for tracking past mangrove ecosystems. *Geochimica et Cosmochimica Acta* 68, 411-422.
- Walsh, E.M., Ingalls, A.E., Keil, R.G., 2008. Sources and transport of terrestrial organic matter in Vancouver Island fjords and the Vancouver-Washington Margin: A multiproxy approach using $\delta^{13}\text{C}_{\text{org}}$, lignin phenols, and the ether lipid BIT index. *Limnology and Oceanography* 53, 1054-1063.
- Weijers, J.W.H., Panoto, E., Van Bleijswijk, J., Schouten, S., Rijpstra, W.I.C., Balk, M., Stams, A.J.M., Sinninghe Damsté, J.S., 2009a. Constraints on the biological source(s) of the orphan branched tetraether membrane lipids. *Geomicrobiology Journal* 26, 402-414.
- Weijers, J.W.H., Schefuß, E., Schouten, S., Sinninghe Damsté, J.S., 2007a. Coupled thermal and hydrological evolution of tropical Africa over the last deglaciation. *Science* 315, 1701-1704.
- Weijers, J.W.H., Schouten, S., Hopmans, E.C., Geenevasen, J.A.J., David, O.R.P., Coleman, J.M., Pancost, R.D., Sinninghe Damsté, J.S., 2006a. Membrane lipids of mesophilic anaerobic bacteria thriving in peats have typical archaeal traits. *Environmental Microbiology* 8, 648-657.
- Weijers, J.W.H., Schouten, S., Schefuß, E., Schneider, R.R., Sinninghe Damsté, J.S., 2009b. Disentangling marine, soil and plant organic carbon contributions to continental margin sediments: A multi-proxy approach in a 20,000 year sediment record from the Congo deep-sea fan. *Geochimica et Cosmochimica Acta* 73, 119-132.
- Weijers, J.W.H., Schouten, S., Spaargaren, O.C., Sinninghe Damsté, J.S., 2006b. Occurrence and distribution of tetraether membrane lipids in soils: Implications for the use of the TEX₈₆ proxy and the BIT index. *Organic Geochemistry* 37, 1680-1693.

- Weijers, J.W.H., Schouten, S., van den Donker, J.C., Hopmans, E.C., Sinninghe Damsté, J.S., 2007b. Environmental controls on bacterial tetraether membrane lipid distribution in soils. *Geochimica et Cosmochimica Acta* 71, 703-713.
- Weijers, J.W.H., Schouten, S., van der Linden, M., van Geel, B., Sinninghe Damsté, J.S., 2004. Water table related variations in the abundance of intact archaeal membrane lipids in a Swedish peat bog. *FEMS Microbiology Letters* 239, 51-56.
- Zell, C., Kim, J.-H., Moreira-Turcq, P., Abril, G., Hopmans, E.C., Bonnet, M.-P., Lima Sobrinho, R., Sinninghe Damsté, J.S., 2013. Disentangling the origins of branched tetraether lipids and crenarchaeol in the lower Amazon River: Implications for GDGT-based proxies. *Limnology and Oceanography* 58, 343-353.
- Zhu, C., Weijers, J.W.H., Wagner, T., Pan, J.-M., Chen, J.-F., Pancost, R.D., 2011. Sources and distributions of tetraether lipids in surface sediments across a large river-dominated continental margin. *Organic Geochemistry* 42, 376-386.

Tables

Table 1: Fractional abundances and indices of brGDGTs and crenarchaeol present in dust sampled along the west coast of equatorial Africa. Roman numerals refer to the GDGT structures in Fig. 1, where IV is crenarchaeol; ‘b.d.’ = below detection limit; ‘-’ indicates that the respective indices are not calculated due to absence of GDGTs.

Dust sample	Latitude	Longitude	GDGT fractional abundance							BIT	MBT'	DC	CBT	
			<i>f</i> (Ia)	<i>f</i> (Ib)	<i>f</i> (Ic)	<i>f</i> (IIa)	<i>f</i> (IIb)	<i>f</i> (IIc)	<i>f</i> (IIIa)					<i>f</i> (IV)
DO13	1.30 N	6.94 W	0.186	0.014	0.018	0.037	<i>b.d.</i>	<i>b.d.</i>	0.012	0.733	0.24	0.82	-	-
DO14	1.32 N	2.86 W	0.152	<i>b.d.</i>	<i>b.d.</i>	<i>b.d.</i>	<i>b.d.</i>	<i>b.d.</i>	<i>b.d.</i>	0.848	0.15	-	-	-
DO15	1.52 N	0.60 W	0.195	0.017	<i>b.d.</i>	0.036	0.015	<i>b.d.</i>	0.015	0.722	0.25	0.76	0.12	0.86
DO16	1.76 N	1.64 E	0.207	<i>b.d.</i>	<i>b.d.</i>	<i>b.d.</i>	<i>b.d.</i>	<i>b.d.</i>	<i>b.d.</i>	0.793	0.21	-	-	-
DO17	2.61 N	6.54 E	0.249	0.039	<i>b.d.</i>	0.067	0.020	<i>b.d.</i>	<i>b.d.</i>	0.625	0.34	0.77	0.16	0.73
DO18	1.68 N	7.97 E	0.153	<i>b.d.</i>	<i>b.d.</i>	0.063	<i>b.d.</i>	<i>b.d.</i>	<i>b.d.</i>	0.784	0.22	0.71	-	-
DO19	1.74 N	9.14 E	0.309	0.025	<i>b.d.</i>	0.062	0.017	<i>b.d.</i>	<i>b.d.</i>	0.587	0.39	0.81	0.10	0.95
DO20	1.65 N	9.11 E	0.229	<i>b.d.</i>	<i>b.d.</i>	<i>b.d.</i>	<i>b.d.</i>	<i>b.d.</i>	<i>b.d.</i>	0.771	0.23	-	-	-
DO21	1.38 S	8.54 E	0.173	0.010	0.004	0.018	0.008	0.002	0.009	0.777	0.20	0.84	0.08	1.04
DO22	2.91 S	9.21 E	0.219	<i>b.d.</i>	<i>b.d.</i>	<i>b.d.</i>	<i>b.d.</i>	<i>b.d.</i>	<i>b.d.</i>	0.781	0.22	-	-	-
DO23	6.18 S	10.05 E	0.368	0.018	0.006	0.027	0.009	<i>b.d.</i>	0.007	0.565	0.42	0.90	0.06	1.16
DO24	8.00 S	11.86 E	<i>b.d.</i>	<i>b.d.</i>	<i>b.d.</i>	<i>b.d.</i>	<i>b.d.</i>	<i>b.d.</i>	<i>b.d.</i>	1.000	-	-	-	-
DO25	10.69 S	12.50 E	0.138	0.029	<i>b.d.</i>	0.039	<i>b.d.</i>	<i>b.d.</i>	<i>b.d.</i>	0.794	0.18	0.81	-	-

Table 2: Fractional abundances and indices of brGDGTs and crenarchaeol present in SPM of surface waters of the Atlantic Ocean along the west coast of equatorial Africa. Volume indicates the amount of water filtered for analysis; roman numerals refer to the GDGT structures in Fig. 1; ‘b.d.’ = below detection limit; ‘-’ indicates that the respective indices are not calculated due to absence of GDGTs.

SPM sample	Latitude	Longitude	Volume (L)	Temperature (°C)	Salinity (‰)	GDGT fractional abundance								BIT	MBT'	DC	CBT
						f(Ia)	f(Ib)	f(Ic)	f(IIa)	f(IIb)	f(IIc)	f(IIIa)	f(IV)				
M56B 2	3.77 S	9.12 E	304	27.3	32.0	0.302	0.021	0.010	0.037	0.003	<i>b.d.</i>	0.004	0.623	0.38	0.88	0.07	1.14
M56B 23	4.81 S	9.91 E	244	28.1	33.5	0.233	0.025	0.014	0.027	0.003	<i>b.d.</i>	<i>b.d.</i>	0.698	0.30	0.90	0.10	0.97
M56B 34	6.28 S	10.47 E	403	27.6	28.0	0.551	0.012	0.005	0.069	0.003	<i>b.d.</i>	0.006	0.353	0.65	0.88	0.02	1.60
M56B 37	9.90 S	10.87 E	304	27.0	36.0	0.389	<i>b.d.</i>	<i>b.d.</i>	0.044	<i>b.d.</i>	<i>b.d.</i>	0.018	0.549	0.45	-	-	-
M56B 43	15.40 S	11.30 E	244	21.6	36.0	0.027	<i>b.d.</i>	<i>b.d.</i>	<i>b.d.</i>	<i>b.d.</i>	<i>b.d.</i>	<i>b.d.</i>	0.973	0.03	-	-	-
M56B 47	18.23 S	11.58 E	111	16.0	35.3	0.002	0.000	<i>b.d.</i>	0.002	<i>b.d.</i>	<i>b.d.</i>	0.001	0.995	0.00	-	-	-
M56B 53	22.99 S	13.17 E	198	18.5	35.3	0.005	<i>b.d.</i>	<i>b.d.</i>	<i>b.d.</i>	<i>b.d.</i>	<i>b.d.</i>	<i>b.d.</i>	0.995	0.01	-	-	-
M56B 57	26.10 S	14.12 E	113	16.2	35.3	0.001	<i>b.d.</i>	<i>b.d.</i>	<i>b.d.</i>	<i>b.d.</i>	<i>b.d.</i>	<i>b.d.</i>	0.999	0.00	-	-	-

Table 3: Fractional abundances and indices of brGDGTs present in distal marine surface sediments. Roman numerals refer to the GDGT structures in Fig. 1; ‘b.d.’ = below detection limit; ‘-’ indicates that the respective indices are not calculated due to absence of GDGTs. Asterisks indicate sediments included in the ‘equatorial Atlantic’ subgroup of marine sediments (cf. Figs. 3 and 4).

Sediment sample	Ocean/Region	Latitude	Longitude	Water depth (m)	GDGT fractional abundance								BIT	MBT'	DC	CBT
					f(Ia)	f(Ib)	f(Ic)	f(IIa)	f(IIb)	f(IIc)	f(IIIa)					
GeoB2212-1	Atlantic Ocean*	4.03 N	25.62 W	5521	0.227	<i>b.d.</i>	<i>b.d.</i>	0.144	<i>b.d.</i>	<i>b.d.</i>	0.629	0.06	0.23	-	-	
GeoB2213-1	Atlantic Ocean*	1.27 N	24.15 W	4323	0.150	0.017	<i>b.d.</i>	0.135	0.040	<i>b.d.</i>	0.658	0.01	0.17	0.17	0.70	
GeoB2707-4	Atlantic Ocean	41.95 S	56.32 W	3167	0.377	0.077	0.035	0.158	0.228	0.071	0.054	0.01	0.49	0.36	0.25	
GeoB2722-2	Atlantic Ocean	47.33 S	58.62 W	2351	0.091	0.103	0.037	0.123	0.454	0.143	0.049	0.00	0.23	0.72	-0.41	
GeoB2723-2	Atlantic Ocean	48.91 S	57.88 W	569	0.246	0.104	0.049	0.129	0.322	0.077	0.073	0.02	0.40	0.53	-0.06	
GeoB2806-6	Atlantic Ocean	37.83 S	53.14 W	3542	0.159	0.160	0.073	0.149	0.292	0.079	0.089	0.01	0.39	0.59	-0.17	
GeoB2809-2	Atlantic Ocean	36.33 S	51.52 W	3539	0.194	0.160	0.072	0.161	0.260	0.068	0.084	0.02	0.43	0.54	-0.07	
GeoB2824-1	Atlantic Ocean	33.50 S	42.50 W	4512	0.172	0.065	0.030	0.161	0.115	0.029	0.428	0.01	0.27	0.35	0.27	
GeoB6407-2	Atlantic Ocean	42.04 S	19.50 W	3384	0.147	0.026	0.010	0.143	0.135	0.035	0.505	0.01	0.18	0.36	0.26	
GeoB6410-1	Atlantic Ocean	44.52 S	20.90 W	4038	0.132	0.028	0.012	0.108	0.103	0.029	0.588	0.01	0.17	0.35	0.26	
GeoB8303-5	Atlantic Ocean*	34.26 S	16.78 E	3447	0.134	0.131	0.068	0.145	0.327	0.094	0.101	0.01	0.33	0.62	-0.21	
GeoB8336-5	Atlantic Ocean*	29.21 S	12.34 E	3626	0.149	0.069	0.033	0.160	0.157	0.043	0.390	0.01	0.25	0.42	0.14	
GeoB8342-5	Atlantic Ocean*	31.50 S	13.00 E	3521	0.143	0.053	<i>b.d.</i>	0.157	0.158	0.049	0.440	0.01	0.20	0.41	0.15	
GeoB9526-4	Atlantic Ocean*	12.43 N	18.06 W	3223	0.175	0.107	0.044	0.131	0.351	0.120	0.072	0.02	0.33	0.60	-0.18	
GeoB9529-1	Atlantic Ocean*	8.35 N	17.37 W	1234	0.326	0.080	0.047	0.198	0.220	0.064	0.065	0.02	0.45	0.36	0.24	
IS-S2	Atlantic Ocean	48.18 N	9.71 W	1035	0.385	0.115	0.069	0.166	0.127	0.045	0.093	0.02	0.57	0.31	0.36	
ENAM9407	Atlantic Ocean	62.96 N	4.03 W	2060	0.408	0.082	0.027	0.146	0.233	0.065	0.039	0.02	0.52	0.36	0.24	
All-GGC-22	Atlantic Ocean	54.79 S	3.33 W	2768	0.377	<i>b.d.</i>	<i>b.d.</i>	<i>b.d.</i>	<i>b.d.</i>	<i>b.d.</i>	0.623	0.03	-	-	-	
T89-32	Atlantic Ocean*	14.97 S	10.67 E	3342	0.356	0.040	<i>b.d.</i>	0.190	0.130	<i>b.d.</i>	0.284	0.07	0.40	0.24	0.51	
T89-40	Atlantic Ocean*	21.62 S	6.78 E	3060	0.173	0.034	<i>b.d.</i>	0.184	0.117	<i>b.d.</i>	0.491	0.01	0.21	0.30	0.37	
NP-07-13-09 ^a	Svalbard	79.07 N	10.67 E	326	0.120	0.149	0.057	0.126	0.274	0.051	0.223	0.02	0.33	0.63	-0.24	
NP-07-13-49 ^a	Svalbard	79.01 N	11.38 E	380	0.123	0.170	0.066	0.113	0.292	0.047	0.189	0.01	0.36	0.66	-0.29	
HS 253	Southern Ocean	75 S	26 W	unknown	0.099	0.051	0.018	0.129	0.168	0.044	0.492	0.02	0.17	0.49	0.02	
GeoB10016-2	Indian Ocean	1.60 N	96.66 E	1900	0.518	0.088	0.053	0.174	0.092	0.028	0.047	0.02	0.66	0.21	0.58	
GeoB10040-3	Indian Ocean	6.48 S	102.86 E	2605	0.346	0.083	0.044	0.127	0.209	0.065	0.126	0.01	0.47	0.38	0.21	
NIOF 902	Indian Ocean	10.78 N	51.58 E	459	0.241	0.118	0.077	0.273	0.091	0.031	0.170	0.03	0.44	0.29	0.39	
NIOF 903	Indian Ocean	10.78 N	51.66 E	789	0.210	0.110	0.072	0.218	0.144	0.035	0.211	0.02	0.39	0.37	0.23	
NIOF 904	Indian Ocean	10.79 N	51.77 E	1194	0.198	0.116	0.068	0.187	0.139	0.043	0.249	0.02	0.38	0.40	0.18	
NIOF 907	Indian Ocean	10.80 N	52.25 E	2807	0.559	<i>b.d.</i>	<i>b.d.</i>	0.441	<i>b.d.</i>	<i>b.d.</i>	<i>b.d.</i>	0.01	-	-	-	
NIOF 908	Indian Ocean	10.78 N	52.92 E	3572	0.193	0.070	0.045	0.151	0.224	0.069	0.247	0.02	0.31	0.46	0.07	
Box 476	Arabian Sea	24.10 N	65.47E	1226	0.140	0.063	0.045	0.178	0.105	0.040	0.430	0.03	0.25	0.35	0.28	
PM1	Peru Margin	11.98 S	77.32 W	100	0.261	0.047	0.026	0.314	0.042	0.005	0.305	0.02	0.33	0.13	0.81	
PM7	Peru Margin	11.05 S	78.07 W	250	0.247	0.037	0.024	0.219	0.050	0.008	0.415	0.03	0.31	0.16	0.73	
F1-3 ^b	East China Sea	30.00 N	123.99 W	63	0.169	0.135	0.111	0.255	0.123	0.050	0.156	0.07	0.42	0.38	0.22	
F4-7 ^b	East China Sea	27.38 N	123.33 W	106	0.144	0.179	0.128	0.139	0.175	0.062	0.172	0.07	0.45	0.56	-0.10	
Cariaco Basin	Caricaco Basin	10.67 N	65.60 W	1460	0.339	0.041	0.023	0.381	0.031	0.008	0.176	0.01	0.40	0.09	1.00	
MC-1	Pacific Ocean	41.30 N	141.55 E	1002	0.177	0.143	0.062	0.182	0.194	0.049	0.194	0.02	0.38	0.48	0.03	

BS 07E Black Sea 43.0 N 34.0 E 1288 0.216 0.117 0.071 0.186 0.177 0.028 0.204 0.02 0.40 0.42 0.13

^a data from Peterse et al. (2009); ^b data from Zhu et al. (2011)

Table 4: Fractional abundances and indices of brGDGTs and crenarchaeol present in surface sediments of the Congo deep sea river fan (from Weijers et al., 2007a). The two anker samples represent grab samples taken from the Congo River estuary (cf. Schefuß et al., 2004). Roman numerals refer to the GDGT structures in Fig. 1; ‘b.d.’ = below detection limit; ‘-’ indicates that the respective indices are not calculated due to absence of GDGTs.

Sample ID	Latitude	Longitude	Water depth (m)	GDGT fractional abundance								BIT	MBT'	DC	CBT
				f(Ia)	f(Ib)	f(Ic)	f(IIa)	f(IIb)	f(IIc)	f(IIIa)	f(IV)				
Anker 24	6.03 S	12.57 E	5	0.712	0.054	0.016	0.140	0.019	0.003	0.015	0.041	0.95	0.82	0.08	1.06
Anker 26	6.05 S	12.48 E	6	0.584	0.062	0.038	0.192	0.026	0.008	0.033	0.056	0.94	0.72	0.11	0.94
T89-12	5.20 S	7.97 E	4068	0.193	0.034	0.009	0.080	0.028	0.003	0.050	0.604	0.35	0.59	0.20	0.64
T89-14	3.51 S	9.69 E	868	0.029	0.004	0.002	0.007	0.007	0.002	0.009	0.939	0.05	0.58	0.29	0.50
T89-15	4.21 S	10.02 E	1930	0.128	0.010	<i>b.d.</i>	0.019	0.018	<i>b.d.</i>	0.015	0.809	0.17	0.73	0.18	0.72
T89-16	5.71 S	11.23 E	826	0.280	0.014	0.005	0.037	0.009	<i>b.d.</i>	0.016	0.638	0.34	0.83	0.07	1.15
T89-19	6.04 S	9.96 E	3140	0.413	<i>b.d.</i>	<i>b.d.</i>	0.047	<i>b.d.</i>	<i>b.d.</i>	<i>b.d.</i>	0.540	0.46	-	-	-
T89-20	7.31 S	11.54 E	1080	0.102	0.005	0.002	0.013	0.007	0.002	0.008	0.861	0.12	0.79	0.10	0.96

Table 5: Average BIT, MBT' and DC indices and CBT ratios of the different sample groups discussed in the text. Numbers in parentheses are standard deviations; 'n.a.' = not applicable since samples were selected based on their BIT index values.

Sample group	BIT	MBT'	DC	CBT
Global soils ^a	0.90 (0.15)	0.49 (0.23)	0.16 (0.15)	0.96 (0.59)
African soils ^a	0.85 (0.20)	0.76 (0.22)	0.13 (0.18)	1.28 (0.79)
Dust filters	0.25 (0.08)	0.80 (0.06)	0.11 (0.04)	0.95 (0.17)
Surface water	0.23 (0.25)	0.89 (0.01)	0.06 (0.04)	1.24 (0.33)
Congo fan	0.42 (0.35)	0.72 (0.10)	0.15 (0.08)	0.85 (0.24)
African Atlantic	n.a.	0.28 (0.10)	0.39 (0.16)	0.21 (0.31)
Global marine	n.a.	0.35 (0.12)	0.40 (0.16)	0.20 (0.32)

^a soils from database in Peterse et al. (2012)

Table 6: Results of the ANOVA pairwise multiple comparison test. Values in bold indicate that the mean difference between the respective sample groups is significant at the 90 % confidence level. Group numbers correspond to the following sample groups (cf. Fig. 4): 1 = global soils, 2 = African soils, 3 = dust, 4 = surface water SPM, 5 = Congo deep sea fan sediments, 6 = low latitude Atlantic Ocean sediments with BIT values <0.08, 7 = global marine sediments with BIT <0.08.

Group	1	2	3	4	5	6
2	1.000	-	-	-	-	-
3	0.465	1.000	-	-	-	-
4	0.525	0.957	0.996	-	-	-
5	1.000	1.000	0.997	0.740	-	-
6	0.086	0.062	0.024	0.011	0.065	-
7	0.000	0.000	0.000	0.000	0.000	1.000

Figure captions

Figure 1: Structures of glycerol dialkyl glycerol tetraethers (GDGTs) referred to in the text

Figure 2: Sample location map: A) sample locations of marine surface sediments; B) sample locations of dust, surface waters and Congo deep sea fan sediments along the equatorial African coast.

Figure 3: Cross plot of the degree of cyclisation (DC) and the methylation index (MBT') of brGDGTs of the different sample groups discussed in the text.

Figure 4: Box plots of DC indices for the different sample groups discussed in the text. Horizontal solid line within the boxes represents the median, gray boxes comprise 50 % of samples and dots beyond the whiskers represent upper- and lowermost 10 % of samples. No whiskers plotted if $n < 10$. The soil data used are those from Peterse et al. (2012). African soils and low latitude Atlantic sediments are subsets of global soils and global marine sediments, respectively. Groups that are statistically significantly different from each other (at 90 % confidence level) are assigned different letters.

Figure 5: Degree of cyclisation (DC index) of brGDGTs in coastal and shelf sediments from the East China Sea (ECS) shelf plotted against water depth, which in the ECS is in general equivalent to distance from the coast. Red triangles indicate sediments shallower than 10 m;

these shallow sediments are generally characterised by high BIT indices (average = 0.86).

Data from Zhu et al. (2011).

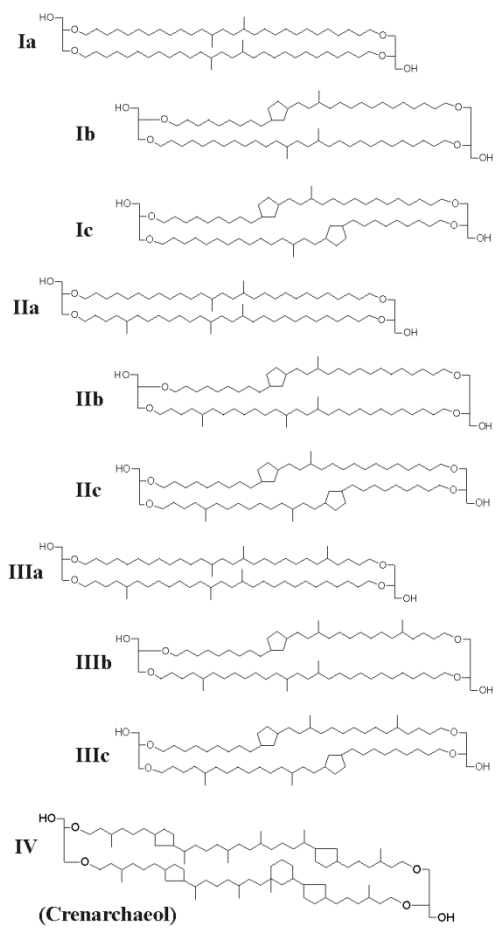


Figure 1

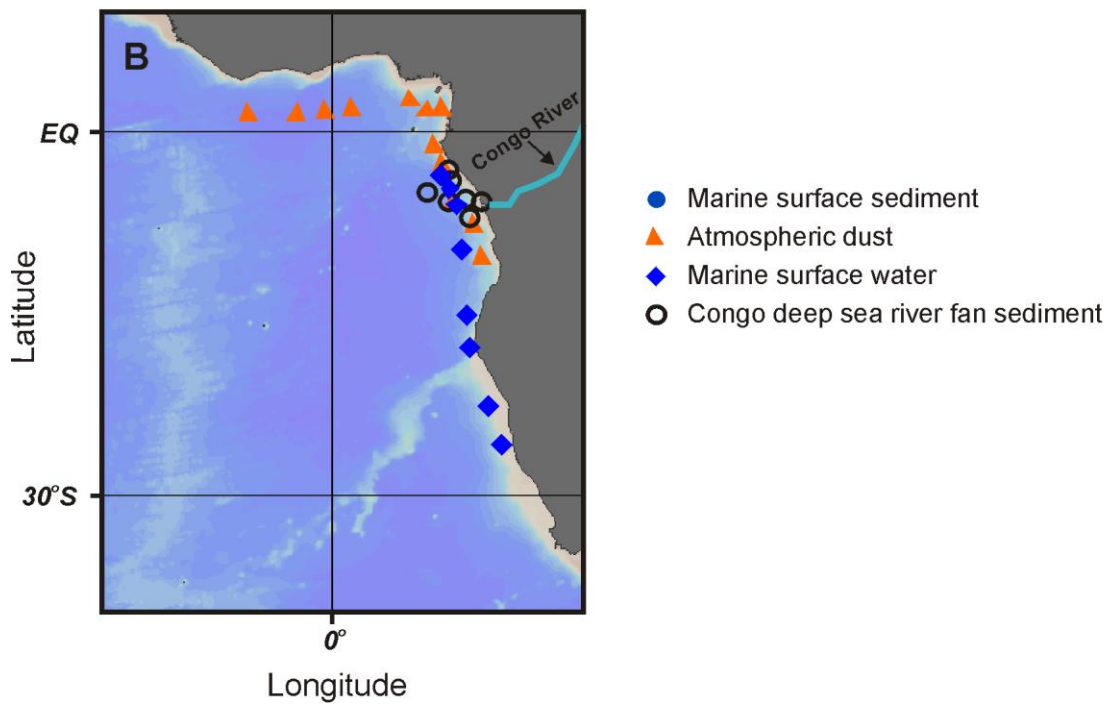
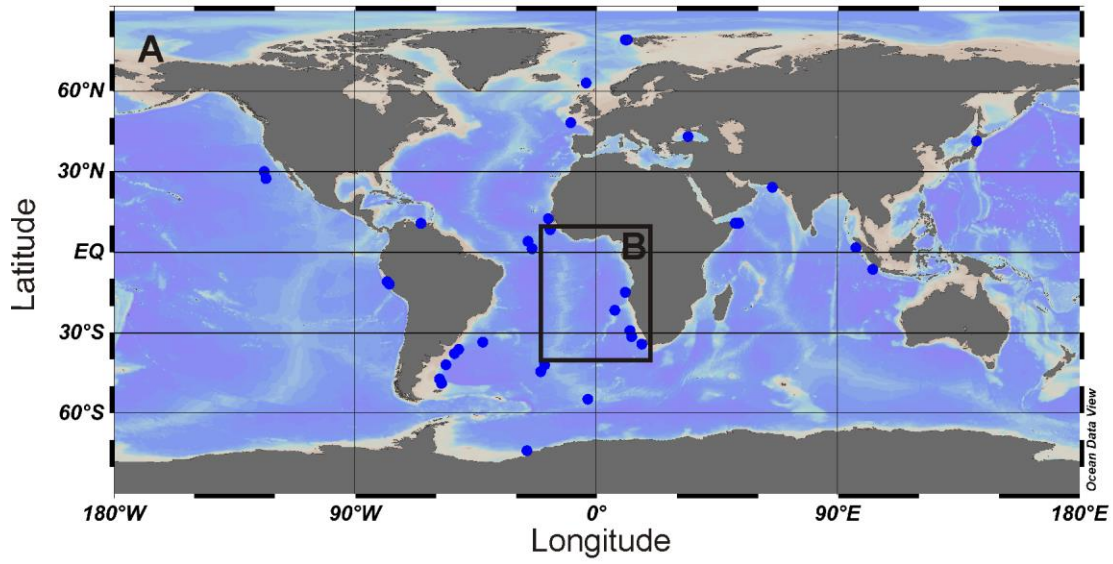


Figure 2

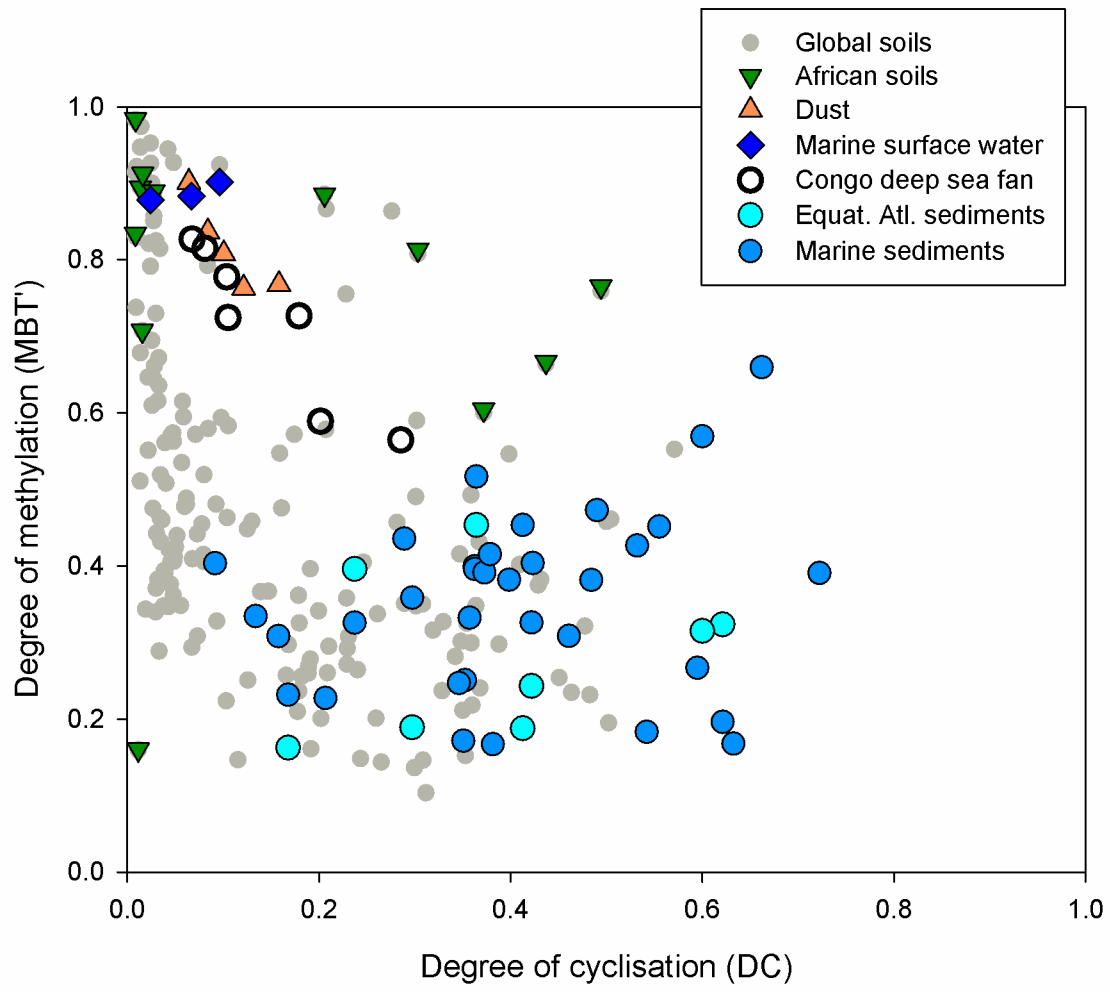


Figure 3

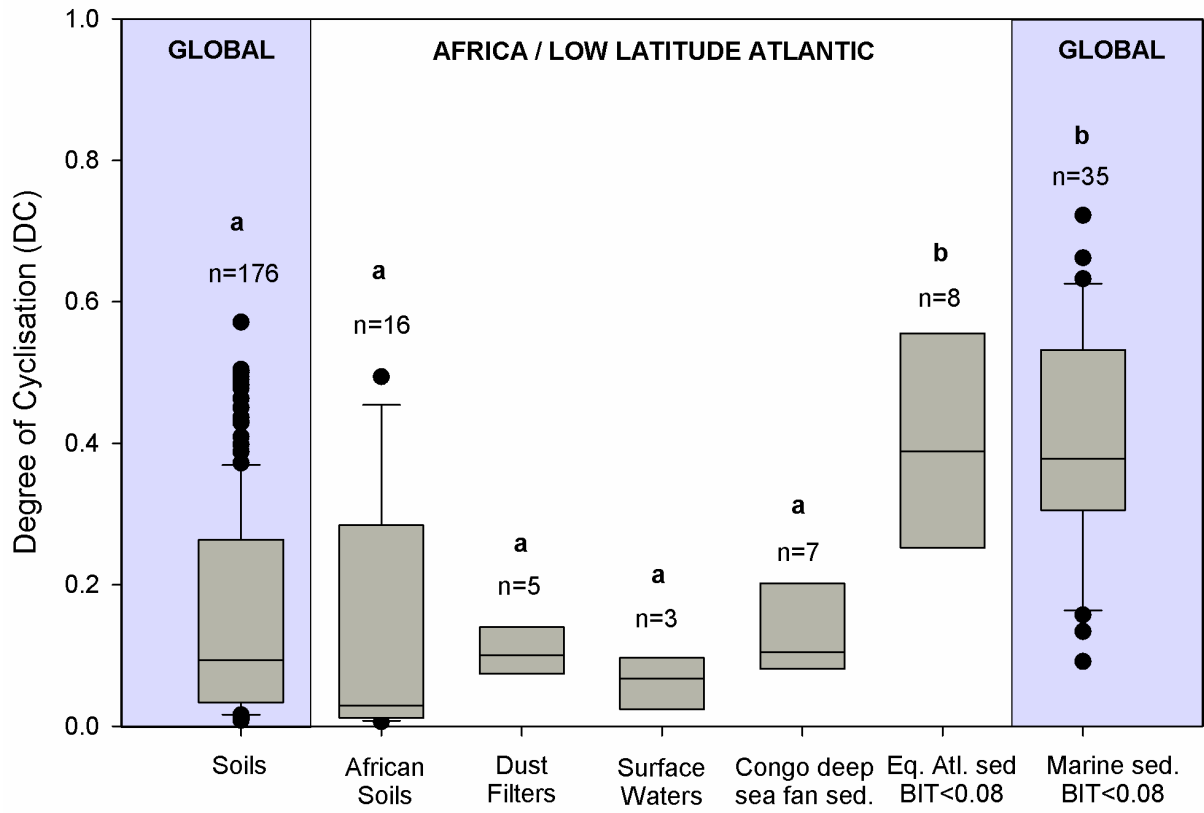


Figure 4

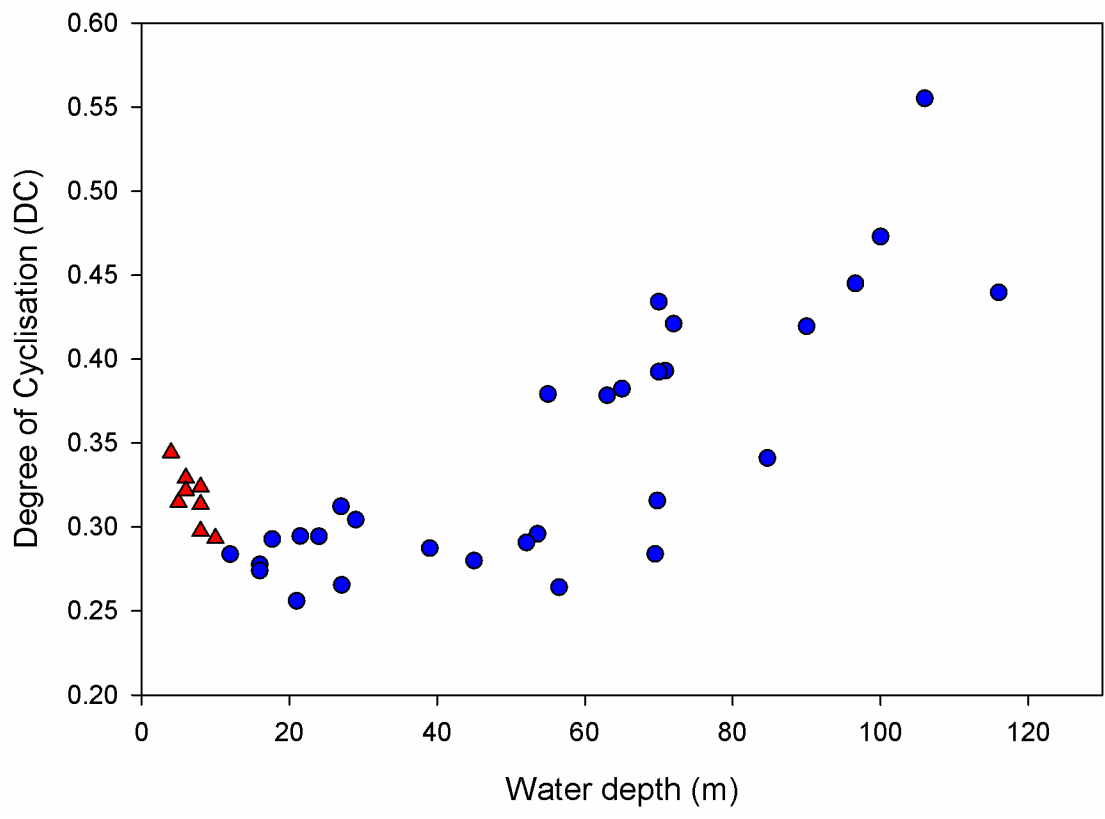


Figure 5